

# Deriving Respiration from the Pulse Photoplethysmographic Signal

Jesús Lázaro<sup>1</sup>, Eduardo Gil<sup>1,2</sup>, Raquel Bailón<sup>1,2</sup>, Pablo Laguna<sup>1,2</sup>

<sup>1</sup>Aragón Institute for Engineering Research (I3A), IIS, University of Zaragoza, Zaragoza, Spain

<sup>2</sup>CIBER de Bioingeniería, Biomateriales y Nanomedicina (CIBER-BBN), Zaragoza, Spain

## Abstract

*A method for respiratory signal estimation from the pulse photoplethysmographic (PPG) signal is presented. The method is based on combination of three parameters present in this signal: pulse rate variability, pulse amplitude variability and pulse width variability.*

*Evaluation is performed over a database containing electrocardiographic (ECG), PPG and respiratory signals simultaneously recorded in 17 subjects during a tilt table test, obtaining a respiratory rate estimation error of  $-0.26 \pm 7.30\%$  ( $-2.11 \pm 14.49$  mHz). These results are comparable or outperform those obtained from other methods which involve the ECG, so it is possible to have reliable respiration estimates from just the PPG.*

## 1. Introduction

Acquiring accurate respiratory signal and frequency rates from a pulse oximeter takes special importance in cases it is necessary to know if a low oxygen saturation reading is due to low respiratory rates or is the result of a low degree of gass exchange in the lungs, which can represent a dangerous physiological condition. Additionally, to have access to the respiratory signal itself is useful, especially for ambulatory analysis or sleep apnea scrutiny.

During expiration, our parasympathetic nervous system makes the blood vessels more flexible than during inspiration. Blood vessels flexibility affects to the propagation velocity of the pulse wave, which at the same time affects the pulse waves width in pulse photoplethysmographic (PPG) signal. In that way, pulse wave width is one parameter present in PPG signal that depends on respiration, so our hypothesis is that respiratory information can be extracted from pulse width variability (PWV). We also complemented respiratory information from pulse amplitude variability (PAV) since respiration also modulates the amplitude of the PPG signal. Another respiration related parameter present in PPG signal is pulse rate variability (PRV). Although pulse rate variability is not an exact surrogate for heart rate variability [1, 2], it is also affected by parasympathetic system and so related to respiration.

For comparison purposes, we also generated other derived respiration (DR) signals which involve electrocardiogram (ECG): pulse transit time (PTT) [3] and rotation angle series of the vectorcardiogram (VCG) loop [4].

Respiratory rate was estimated using an spectrum-based algorithm based on [4]. It was estimated from PWV, PAV, PRV and PTT separately, and combining the three PPG-based signals and also the three rotation angles series.

## 2. Methods

### 2.1. Data and signal preprocessing

The database signals were recorded during a tilt table test from 17 volunteers (11 men and 6 women) whose age is  $28.5 \pm 2.5$  according to the following protocol: 4 min in early supine position, 5 min tilted head-up to an angle of  $70^\circ$  and 4 min back to later supine position. Table takes 18 s to tilt during transitions.

The PPG signal was recorded from index finger with a sampling rate of 250 Hz, whereas the standard ECG leads I, III and the six precordials were recorded with a sampling rate of 1000 Hz, and the respiratory signal was recorded with a sampling rate of 125 Hz. Standard ECG lead II was obtained by the sum of I and III leads, and vectorcardiogram (VCG) was synthesized using the inverse Dower matrix.

The preprocessing applied to the PPG signal consists of a low-pass filtering with a cutoff frequency of 35 Hz. In the ECG, the baseline was removed with a high-pass filter with a cutoff frequency of 0.3 Hz, and the 50 Hz interference was considerably attenuated with the non-linear technique described in [5]. Then, beats from ECG and pulses from PPG were detected to generate derived respiratory (DR) signals. The location of each R-wave in the ECG ( $n_{R_i}$ ) and each pulse apex ( $n_{A_i}$ ) and basal ( $n_{B_i}$ ) points in PPG were automatically determined using the algorithm described in [2]. Artifactual PPG pulses were suppressed by using the artefact detector described in [6].

For the onset and end of pulse waves detection in PPG, we adapted the algorithm presented in [7] which was originally designed for detecting the wave boundaries in ECG

signals. The algorithm uses a low-pass derivative

$$x'_{\text{PPG}}(n) = x_{\text{PPGLP}}(n) - x_{\text{PPGLP}}(n-1) \quad (1)$$

where  $x_{\text{PPGLP}}(n)$  is the low-pass filtered signal with cut-off 5 Hz using a zero-phase forward/backwards digital filtering technique over PPG signal ( $x_{\text{PPG}}(n)$ ).

For the  $i^{\text{th}}$  pulse wave, the algorithm uses the maximum upslope point ( $n_{U_i}$ )

$$n_{U_i} = \arg \max_n x'_{\text{PPG}}(n), \quad n \in [n_{A_i} - 0.3f_s, n_{A_i}] \quad (2)$$

Then, the pulse wave onset  $n_{O_i}$  is estimated as: If  $x'_{\text{PPG}}(n)$  falls down by a threshold ( $\eta = 0.15$ ) dependent value of the maximum upslope  $x'_{\text{PPG}}(n_{U_i})$  anywhere in  $\Omega_{O_i}$ ,

$$\Omega_{O_i} = [n_{A_i} - 0.3f_s, n_{U_i}] \quad (3)$$

then

$$n_{O_i} = \arg \min_{n \in \Omega_{O_i}} \{|x'_{\text{PPG}}(n) - \eta x'_{\text{PPG}}(n_{U_i})|\} \quad (4)$$

Else if there exists any local minimum in  $x'_{\text{PPG}}(n)$  within  $\Omega_{O_i}$  time interval, then  $n_{O_i}$  is set as the last one of those local minima. Otherwise, when no local minimum is found, then  $n_{O_i}$  is set as the sample when minimum value of  $x'_{\text{PPG}}(n)$  occurs within  $\Omega_{O_i}$ .

Pulse wave ends  $n_{E_i}$  were detected in a similar way as  $n_{O_i}$  but using maximum downslope ( $n_{D_i}$ ) instead of  $n_{U_i}$ , in the interval  $[n_{A_i}, n_{A_i} + 0.3f_s]$  and  $\Omega_{E_i} = [n_{D_i}, n_{A_i} + 0.3f_s]$ . Figure 1 in section 2.2 illustrates the significant points of this algorithm.

## 2.2. Derived respiration signals

The PWV-based derived respiration (DR) signal is defined as

$$d_{\text{PWV}}^u(n) = \sum_i (n_{E_i} - n_{O_i}) \delta(n - n_{A_i}) \quad (5)$$

where the superscript “ $u$ ” denotes that the signal is unevenly sampled, see Figure 1.

PAV-based DR signal is defined as

$$d_{\text{PAV}}^u(n) = \sum_i [x_{\text{PPG}}(n_{A_i}) - x_{\text{PPG}}(n_{B_i})] \delta(n - n_{A_i}) \quad (6)$$

and we used the inverse interval function for PRV-based DR, defined as:

$$d_{\text{PRV}}^u(n) = \sum_i \frac{1}{n_{A_i} - n_{A_{i-1}}} \delta(n - n_{A_i}). \quad (7)$$

For this study, pulse transit time (PTT) signal was defined as the time interval between the R peak ( $n_{R_i}$ ) on the

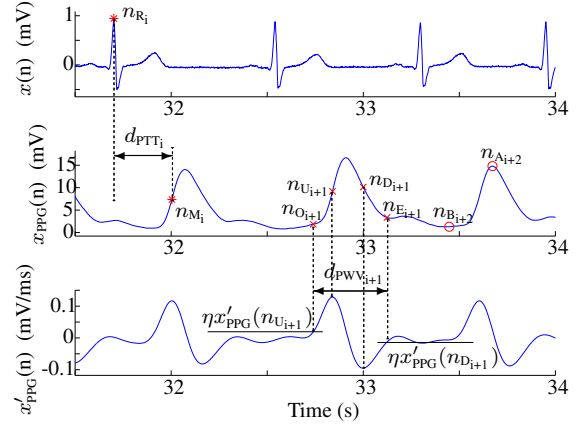


Figure 1. Significant points of this study and definitions for PWV and PTT.  $x(n)$  denotes lead V4 of ECG signal.

lead V4 of ECG signal and the instant when pulse wave on PPG rises by 50% the value from onset to maximum amplitude, ( $n_{M_i}$ ), and illustrated in Figure 1.

$$d_{\text{PTT}}^u(n) = \sum_i (n_{M_i} - n_{R_i}) \delta(n - n_{R_i}) \quad (8)$$

Electrical axis is another parameter influenced by respiration. We estimated the electrical rotation angle series using the algorithm described in [4]. All three rotation angle series were considered as DR signals and denoted as  $d_{\phi_x}^u(n)$ ,  $d_{\phi_y}^u(n)$  and  $d_{\phi_z}^u(n)$ .

Finally, we obtained a 4 Hz evenly sampled version of each DR signal by cubic splines interpolation, and filtered with a band-pass filter (0.075-1) Hz. The resulting signals, denoted without the superscript “ $u$ ”,  $d_{\text{PWV}}(n)$ ,  $d_{\text{PRV}}(n)$ ,  $d_{\text{PAV}}(n)$ ,  $d_{\text{PTT}}(n)$ ,  $d_{\phi_x}(n)$ ,  $d_{\phi_y}(n)$  and  $d_{\phi_z}(n)$  are the 4 Hz evenly sampled band-pass filtered versions.

## 2.3. Respiratory rate estimation

The frequency rate estimation algorithm is based on the one presented in [4]. It allows estimating the frequency rate from up to  $N$  DR signals, combining them in order to increase robustness.

For power spectrum estimation, we used the Welch periodogram. Running power spectra of each DR signal used in combination are normalized in the band  $[0, 1]$  Hz and, as in [4], spectra are averaged in order to reduce the variance. For the  $j^{\text{th}}$  DR signal and  $k^{\text{th}}$  running interval of  $T_s$ -s length, the power spectrum  $S_{j,k}(f)$  results from averaging the power spectra obtained from subintervals of length  $T_m$  s ( $T_m < T_s$ ) using an overlap of  $T_m/2$  s. A  $T_s$ -s spectrum is estimated every  $t_s$  s.

For each  $S_{j,k}(f)$ , the location of largest peak  $f_p^1(j, k)$  is detected. Then, a reference interval  $\Omega_R(k)$  is established

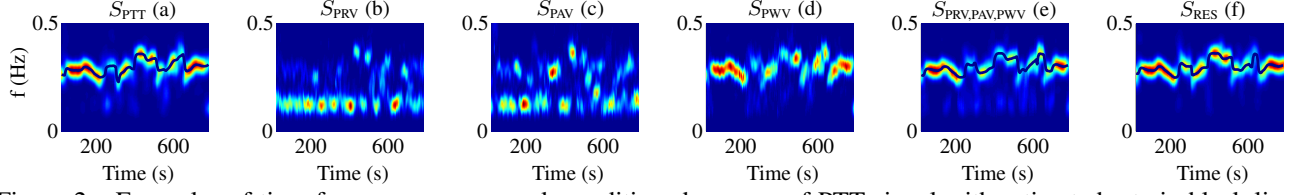


Figure 2. Examples of time-frequency maps: peak-conditioned average of PTT signal with estimated rate in black line (a); PRV Welch periodograms (b); PAV Welch periodograms (c); PWV Welch periodograms (d); peak-conditioned average combining PRV, PAV and PWV with estimated rate in black line (e); peak-conditioned average of reference respiratory signal with estimated rate in black line (f).

as:

$$\Omega_R(k) = [f_R(k-1) - \delta, f_R(k-1) + 2\delta] \quad (9)$$

where  $f_R(k-1)$  is a respiratory frequency reference obtained from previous  $(k-1)$  steps and defines the location of  $\Omega_R(k)$ .  $\Omega_R(k)$  is asymmetric with respect to  $f_R(k-1)$  because the most important contamination present in power spectra is in LF band due to the sympathetic nervous system activity.

All peaks at least larger than 75% of  $f_p^l(j, k)$  inside  $\Omega_R(k)$  are detected, and  $f_p^u(j, k)$  is chosen as the nearest to  $f_R(k-1)$ . Note that  $f_p^u(j, k)$  can be the same  $f_p^l(j, k)$  if the largest peak is also the nearest to  $f_R(k-1)$ .

Then,  $L_s$  spectra  $S_{j,k}(f)$  are “peak-conditioned” averaged; only those  $S_{j,k}(f)$  which are sufficiently peaked take part in the averaging. In this paper, “peaked” is synonymous to that exists  $f_p^u(j, k)$  and a certain percentage ( $\xi$ ) of the spectral power must be contained in an interval centered around it. Peak-conditioned averaging is defined in (10).

$$\bar{S}_k(f) = \sum_{l=0}^{L_s-1} \sum_j \chi_{j,k-l}^A \chi_{j,k-l}^B S_{j,k-l}(f) \quad (10)$$

where  $\chi_{j,k-l}^A$  and  $\chi_{j,k-l}^B$  represent two criteria referred to decide if power spectrum  $S_{j,k-l}(f)$  is peaked enough or not, as shows the equations 11 and 12.

$$\chi_{j,k}^A = \begin{cases} 1, & P_{j,k} \geq \xi \\ 0, & otherwise \end{cases} \quad (11)$$

$$\chi_{j,k}^B = \begin{cases} 1, & P_{j,k} \geq \lambda \max_{i \neq j} \{P_{i,k}\} \\ 0, & otherwise \end{cases} \quad (12)$$

where  $P_{j,k}$  is defined by

$$P_{j,k} = \frac{\int_{f_p^u(j,k)-0.6\delta}^{f_p^u(j,k)+0.6\delta} S_{j,k}(f) df}{\int_{f_R(k-1)-\delta}^{f_R(k-1)+2\delta} S_{j,k}(f) df} \quad (13)$$

In the averaged spectrum  $\bar{S}_k(f)$  the algorithm also searches the largest peak (denoted  $f_p^{1a}(k)$ ) and  $f_p^{u_a}(k)$  as

the nearest to  $f_R(k-1)$  inside the interval  $\Omega_R(k)$  which is at least larger than 75% of  $f_p^{1a}(k)$ . At this time the reference frequency  $f_R(k)$  can be updated as:

$$f_R(k) = \beta f_R(k-1) + (1-\beta) f_p(k) \quad (14)$$

where  $\beta$  denotes the forgetting factor and  $f_p(k)$  is defined by

$$f_p(k) = \begin{cases} f_p^{u_a}(k), & \exists f_p^{u_a}(k) \\ f_p^{1a}(k), & otherwise \end{cases} \quad (15)$$

Finally, estimated respiration rate  $\hat{f}(k)$  is defined as:

$$\hat{f}(k) = \alpha \hat{f}(k-1) + (1-\alpha) f_p(k) \quad (16)$$

$$\alpha = \begin{cases} \alpha_2, & \exists f_p^{u_a}(j, k) \\ \alpha_1, & otherwise \end{cases} \quad (17)$$

where  $\alpha_2 \leq \alpha_1$ , providing more memory when  $f_p^{u_a}(k)$  could not be set.

Note that  $\bar{S}_k(f)$  is the result of an averaging from zero up to  $N \times L_s$  power spectra. If no spectrum took part in the average, the algorithm increases the reference interval by doubling  $\delta$  value and repeat the process from the search of  $f_p^l(j, k)$  and  $f_p^u(j, k)$  in individual power spectra. In the case that no spectrum is peaked enough after this second iteration,  $f_R(k)$  and  $\hat{f}(k)$  are set as previous  $f_R(k-1)$  and  $\hat{f}(k-1)$ , respectively.

At initialization time, in order to reduce the risk of spurious frequency selection  $\delta$  is set to 0.125 Hz and  $f_R(0)$  is set to 0.275 Hz, allowing algorithm to pick peaks inside [0.15, 0.525] Hz band. Occasionally, there are some subjects in our data base whose respiratory rate is below 0.15 Hz so algorithm can not be initialized as proposed. To solve that issue, if  $f_R$  is not set after 5 averages  $\bar{S}_k(f)$ , then  $\delta$  is increased allowing algorithm to pick peaks in full [0, 1] Hz studied band.

Concatenation of all  $\bar{S}_k(f)$  results in a time-frequency map  $\bar{S}(k, f)$  where the LF contamination is considerably reduced, as shown in Figure 2. The following parameters were used:  $L_s = 5$ ,  $T_s = 40s$ ,  $T_m = 12s$ ,  $\xi = 0.5$ ,  $\delta = 0.08Hz$ ,  $\lambda = 0.95$ ,  $\beta = 0.8$ ,  $\alpha_1 = 0.7$  and  $\alpha_2 = 0.3$ .

	PWV		PAV		PRV		P <sub>COMB</sub>		PTT		φ <sub>COMB</sub>	
	mean	std	mean	std	mean	std	mean	std	mean	std	mean	std
$f_{RES} \geq 0.15Hz$	-1.03	6.79	-25.19	19.63	-22.87	16.58	-1.19	5.40	-3.37	9.14	0.71	5.00
$f_{RES} < 0.15Hz$	5.21	14.28	2.33	17.13	4.92	13.07	1.45	10.79	6.71	15.80	3.55	11.89
<b>All</b>	<b>1.17</b>	<b>9.44</b>	<b>-15.45</b>	<b>18.75</b>	<b>-13.07</b>	<b>15.34</b>	<b>-0.26</b>	<b>7.30</b>	<b>0.19</b>	<b>11.49</b>	<b>1.72</b>	<b>7.43</b>

Table 1. Intersubject means of mean (*mean*) and standard deviation (*std*) of  $e(k)$  signal in percentage. P<sub>COMB</sub> refers to the combination of DR signals  $d_{PWV}(n)$ ,  $d_{PRV}(n)$  and  $d_{PAV}(n)$ . φ<sub>COMB</sub> refers to the combination of all three rotation angle series.

### 3. Results

We estimated the respiration rate from  $d_{PWV}(n)$ ,  $d_{PRV}(n)$  and  $d_{PAV}(n)$  separately, meaning no average in  $j^{th}$  in (10), and also combining them. We also obtained an estimated rate from  $d_{PTT}(n)$  and from combination of all three rotation angle series ( $d_{\phi_x}(n)$ ,  $d_{\phi_y}(n)$  and  $d_{\phi_z}(n)$ ) and, finally, applied the algorithm to the reference respiratory signal  $r(n)$  in order to evaluate them. We will denote  $\hat{f}_d(k)$  the estimated frequency rate from DR signal  $d$ , and  $\hat{f}_{RES}(k)$  the one estimated from  $r(n)$ . We computed a relative error signal  $e(k)$  defined as:

$$e(k) = \frac{\hat{f}_d(k) - \hat{f}_{RES}(k)}{\hat{f}_{RES}(k)} \times 100 \quad (18)$$

Then, we removed samples of  $e(k)$  corresponding to the time intervals between parts of tilt table test (rest-tilt-rest) and computed mean and standard deviation. Results are shown in Table 1.

### 4. Discussion and conclusions

In this paper a method for the estimation of respiratory rate from the PPG signal has been presented. We have used three different kinds of information: PAV, PRV, and the innovative PWV. Rate estimation method is based on the one proposed in [4] but includes spectrum normalization and a redefinition of “peak-conditioned” average, both aimed to deal with combining DR signals with different origin.

On the evaluation over the database the method obtained a mean respiratory rate error of  $-0.26 \pm 7.30\%$  ( $-2.11 \pm 14.49$  mHz) and, separating registers into  $\hat{f}_{RES} \geq 0.15Hz$  and  $\hat{f}_{RES} < 0.15Hz$ , the method obtained a mean rate error of  $-1.19 \pm 5.40\%$  ( $-3.65 \pm 15.13$  mHz) and  $1.45 \pm 10.79\%$  ( $0.71 \pm 13.31$  mHz), respectively.

PWV showed better performance than other single DR signals in respiratory rate error terms, and combination of PWV, PAV and PRV DR signals improved results even the ones obtained with PTT or rotation angle series, which involve ECG registration. These results allow to derive respiration from PPG (no need of ECG) useful for ambulatory analysis and for sleep apnea scrutiny due to the simplicity of PPG recordings.

### Acknowledgements

This work is supported by Ministerio de Ciencia y Tecnología, FEDER; under project TEC2010-21703-C03-02, by CIBER de Bioingeniería, Biomateriales y Nanomedicina through Instituto de Salud Carlos III, by ARAID and Ibercaja under Programa de APOYO A LA I+D+i and by Grupo Consolidado GTC from DGA.

### References

- [1] Constant I, Laude D, Murat I, Elghozi JL. Pulse rate variability is not a surrogate for heart rate variability. *Clinical Science* 1999;97(4):391–397.
- [2] Gil E, Orini M, Bailón R, Vergara JM, Mainardi L, Laguna P. Photoplethysmography pulse rate as a surrogate measurement of heart rate variability during non-stationary conditions. *Physiological Measurement* 2010;31:1271–1290.
- [3] Chua CP, Heneghan C. Pulse transit time-derived respiratory parameters and their variability across sleep stages. *Engineering in Medicine and Biology Society* 2005;27:6153–6156.
- [4] Bailón R, Sörnmo L, Laguna P. A robust method for ecg-based estimation of the respiratory frequency during stress testing. *IEEE transactions on biomedical engineering* 2006; 53(7):1273–1285.
- [5] Hamilton PS. A comparison of adaptive and nonadaptive filters for the reduction of powerline interference in the ecg. *IEEE Transactions on Biomedical Engineering* 1996; 43:105–109.
- [6] Gil E, Vergara JM, Laguna P. Detection of decreases in the amplitude fluctuation of pulse photoplethysmography signal as indication of obstructive sleep apnea syndrome in children. *Biomedical Signal Processing and Control* 2008; 3:267–277.
- [7] Laguna P, Jané R, Caminal P. Automatic detection of wave boundaries in multilead ECG signals: validation with the CSE database. *Computers and Biomedical Research* 1994; 27:45–60.

Address for correspondence:

Jesús Lázaro  
 Dep. Ingeniería Electrónica y Comunicaciones. Universidad de Zaragoza, C/ María de Luna 1, 50018 Zaragoza, Spain.  
 jlazarop@unizar.es